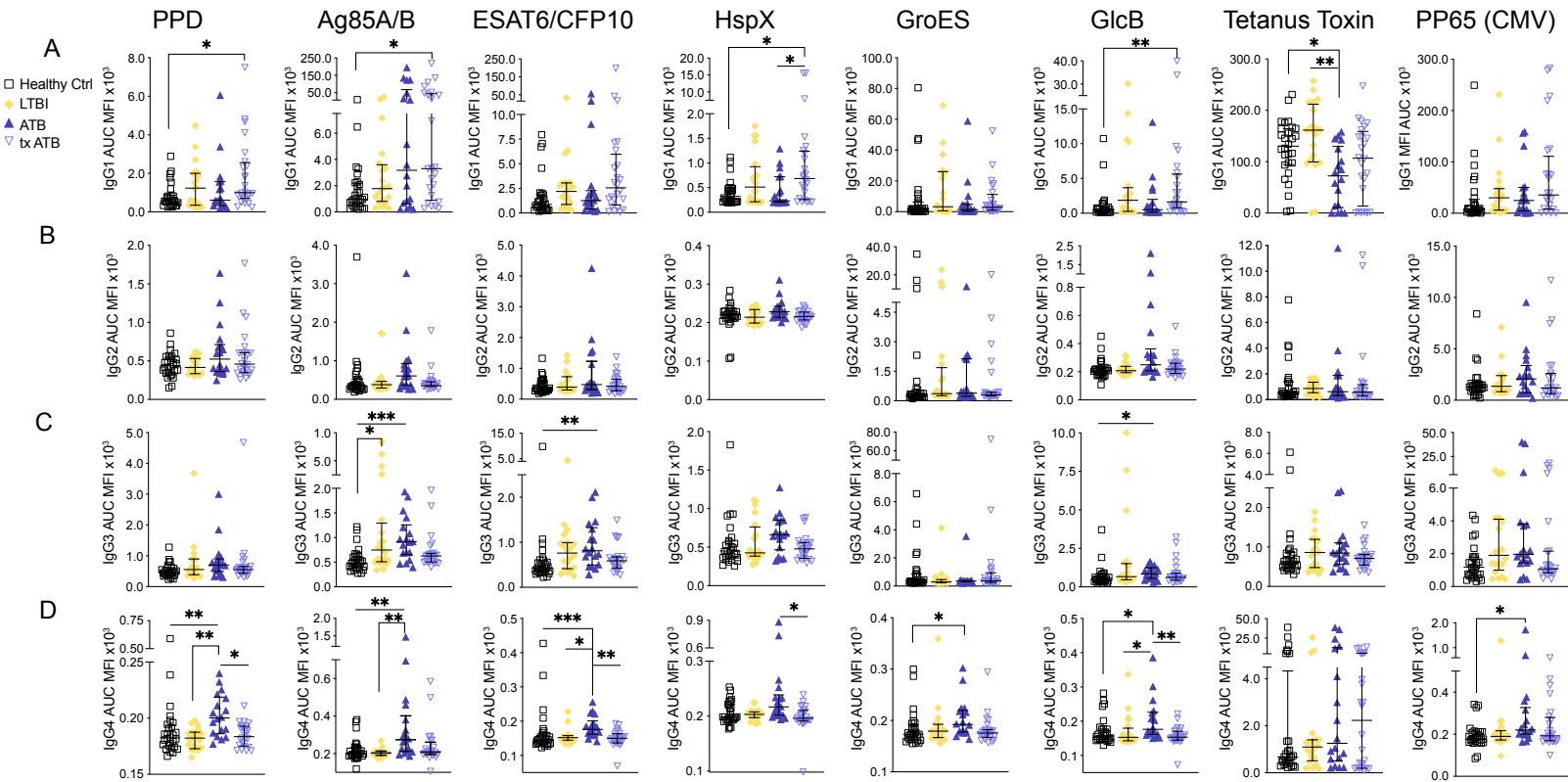
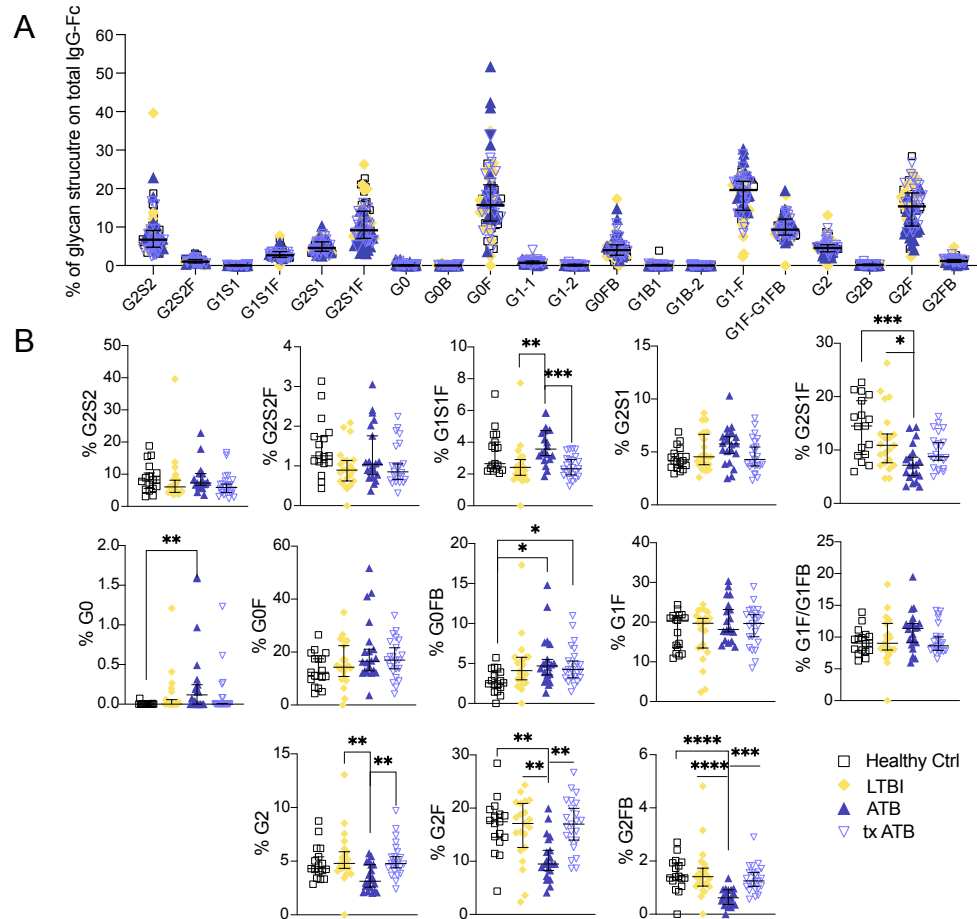


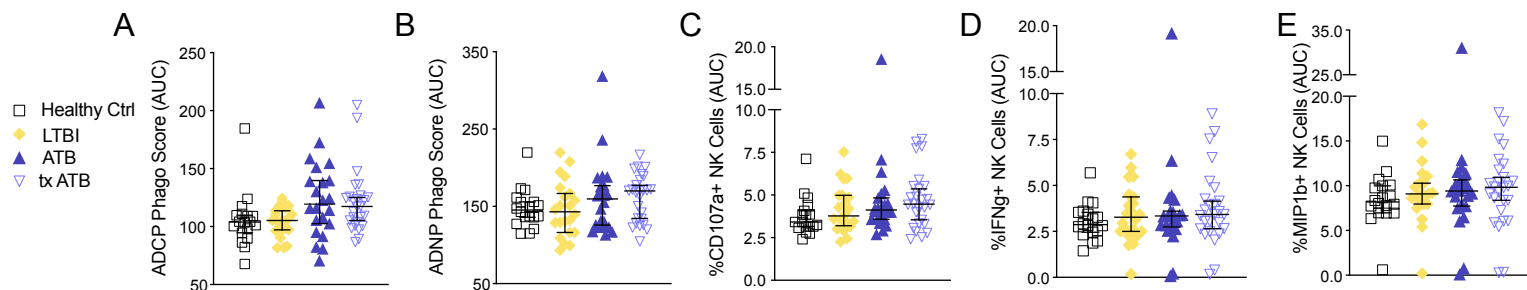
Supplemental Figure 1: Total plasma and antigen-specific isotype titers of cohort individuals. (A) Total serum IgG1, IgG2, IgG3, IgG4, IgM, and IgA quantified with Luminex and total IgG quantified in an ELISA. Antigens PPD, Ag85A/B, ESAT6/CFP10, Tetanus Toxin and FluHA were used in a customized Luminex assay for to measure antigen-specific titers of (B) total IgM, (C) total IgG, (D) total IgA1, and (E) total IgA2. Plasma samples were diluted at 1:30, 1:100, 1:300, and 1:1000 and assayed for binding on antigen specific beads and area under the curve was generated for each antigen:isotype measure made per individual sample. Univariate plots (A-E) represent median and interquartile range of values measured in healthy control (n= 17, black open squares) LTBI (n=21, yellow diamonds), ATB (n=20, blue triangles), and txATB (n=23, periwinkle open triangles) individuals. Kruskal-Wallis test followed by Dunn's correction for multiple tests used to compare healthy control, LTBI, ATB, and txATB individuals: *p<0.05 and **p<0.01.



Supplemental Figure 2: Antigen-specific IgG subclass titers. Titer levels against antigens PPD, Ag85A/B, ESAT6/CFP10, HspX, GroES, GlcB, Tetanus Toxin and CMV-pp65 were measured via Luminex for (A) total IgG1, (B) total IgG2, (C) total IgG3, and (D) total IgG4. Plasma samples were diluted at 1:30, 1:100, and 1:300 and assayed for binding on antigen specific beads and area under the curve was generated for each antigen:isotype measure made per individual sample. Univariate plots (A-D) represent median and interquartile range of the measures from healthy control (n= 17, black open squares) LTBI (n=21, yellow diamonds), ATB (n=20, blue triangles), and txATB (n=23, periwinkle open triangles) individuals. Kruskal-Wallis test followed by Dunn's correction for multiple tests used to compare healthy control, LTBI, ATB, and txATB individuals: *p<0.05, **p<0.01, and ***p<0.005

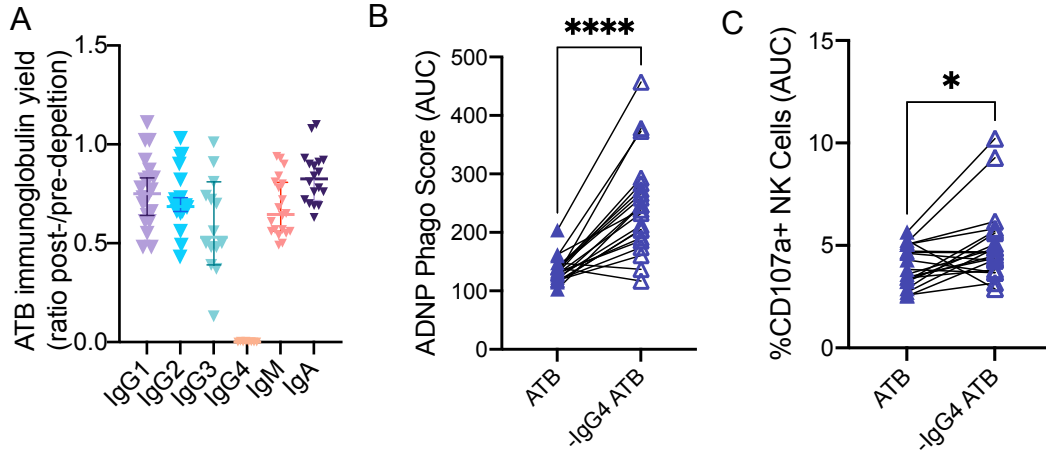


Supplemental Figure 3: Total IgG-Fc glycans. APTS-labelled N-linked glycan structures of the IgG-Fc measured by CE analysis. **(A)** Relative frequencies of measured glycans detectable by prelabelled standards demonstrate that a subset of detected glycans are differentially enriched across all individuals. Univariate plots **(B)** represent glycans measured with medians above 0% in healthy controls (n=17, black open squares), LTBI (n=21, yellow diamonds), ATB (n=20, blue triangles), or txATB (n=22, periwinkle open triangles) individuals. Data plotted as median and interquartile range of the measured values and statistical significance was calculated using Kruskal-Wallis test followed by Dunn's correction for multiple tests: *p<0.05, **p<0.01, ***p<0.005, and ****p<0.001.

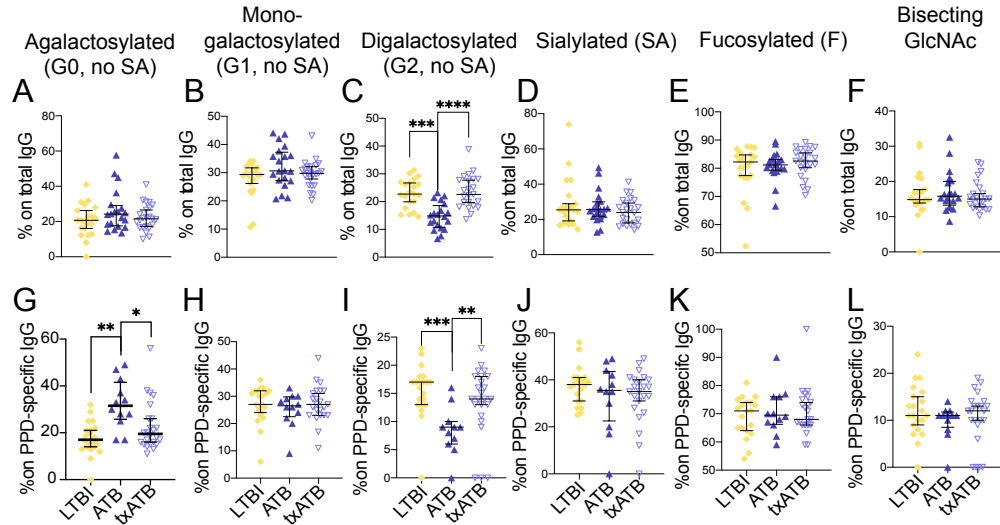


Supplemental Figure 4: Innate immune cell functional responses to plasma antibodies.

Plasma from healthy control (n=17, black open squares), LTBI (n=21, yellow diamonds), ATB (n=20, blue triangles), and txATB (n=23, periwinkle open triangles) individuals were tested for FcR functional activity on innate immune cells. Biotin-PPD coated 1 μ m streptavidin beads were combined with plasma at 1:30, 1:100, and 1:300 dilutions to form immune complexes; these complexes were combined with THP1 cells to measure antibody-dependent cellular phagocytosis (ADCP) (A). Neutrophils isolated from healthy donors were also combined with immune complexes to measure antibody-dependent neutrophil phagocytosis (ADNP) (B), n=6 replicates averaged for a composite AUC phago score. The ability of these plasma samples to induce NK cell degranulation and activation of PPD-specific antibodies bound to ELISA plates was determined by the frequencies of (C) CD107a+ (D) IFN γ + and (E) MIP1 β + NK cells. Data in (C-D) represent an average of signal measured in a minimum of 3 independent donors. AUC for each donor test was generated from plasma dilutions of 1:30, 1:100, and 1:300. No statistically significant difference was found between healthy controls, LTBI, ATB, and txATB using Kruskal-Wallis test followed by Dunn's correction for multiple tests.



Supplemental Figure 5: *IgG4* depletion in *ATB* serum increases antibody function on human neutrophils and NK cells. Serum was depleted of *IgG4* and tested for antibody mediated function in Neutrophils and NK Cells. **(A)** Recovery of antibody isotypes and subclasses following *IgG4* depletion. **(B)** PPD-specific antibodies in serum with and without *IgG4* depletion were tested for function in an Antibody-Dependent Neutrophil Phagocytosis (ADNP), data are representative of n=2 independent healthy neutrophil donors. **(C)** PPD-specific antibodies in serum with and without *IgG4* was tested for the CD107a expression on NK cells (degranulation induction). Data are representative of n=3 independent healthy NK cell donors. Scores for *IgG4* depleted samples are corrected for loss of totaled immunoglobulins following depletion. Statistical significance was calculated using a Mann-Whitney : *p<0.05 and **** p<0.001.



Supplemental Figure 6: Antigen-specific IgG glycans are enriched for additional features distinct from total IgG-Fc glycans that distinguish LTBI and txATB individuals from ATB. Individual glycan structures identified by CE on bulk IgG-Fc (A-F) and PPD-specific IgG-Fc (G-L) were totaled into the major categories of (A, G) agalactosylated structures (G0; all structures lacking galactose), (B, H) mono-galactosylated structures (G1; all structures containing a single galactose), (C, I) digalactosylated structures (G2; all structures containing two galactose structures), (D, J) sialylated structures (SA; all structures with at least one sialic acid), (E, K) fucose (all structures containing fucose), and (F, L) bisecting N-acetylglucosamine (GlcNAc-B; all structures containing a bisecting GlcNAc). Univariate plots (A-F) represent LTBI (n=21, yellow diamonds), ATB (n=20, blue triangles), and txATB (n=23, periwinkle open triangles) individuals. Univariate plots of antigen-specific glycans (G-L) represent a subset of the cohort; LTBI (n=18), ATB (n=11), and txATB (n=26). Statistical significance between LTBI, ATB and txATB were calculated using Kruskal-Wallis test followed by Dunn's correction for multiple tests: *p<0.05, **p<0.01, ***p<0.0005, and **** p<0.0001.